ABUAD Journal of Engineering Research and Development (AJERD)
ISSN (online): 2645-2685; ISSN (print): 2756-6811

Volume 7, Issue 2, 260-269

Circular Microstrip Antennas in 5G: Evaluating Metamaterial Integration

Israel Adeolu OLUWAFEMI[1], Ubong UKOMMI[1], Emmanuel UBOM[1], Akanniyene OBOT[2]

[1]*Department of Electrical and Electronic Engineering, Akwa Ibom State University, Nigeria*
iaoluwafemi@gmail.com/ubongukommi@aksu.edu.ng/emmanuelubom@aksu.edu.ng

[2]*Department of Electrical and Electronic Engineering, University of Uyo, Nigeria*
akaninyeneobot@uniuyo.edu.ng

Corresponding Author: iaoluwafemi@gmail.com, *+2347034658770*
Date Submitted: *09/08/2024*
Date Accepted: *06/09/2024*
Date Published: *14/09/2024*

Abstract: *The rapid emergence of Fifth-Generation (5G) technologies necessitate the development of highly efficient antenna systems with compact design that can support Ultra-Wideband (UWB) frequencies. This work presents the design and enhancement of a Circular Microstrip Antenna (CMSA) for 5G UWB applications using metamaterials. The study focuses on the design of CMSA and the integration of a Complementary Split-Ring Resonator (CSRR) into the circular patch of the CMSA. The design is simulated using Computer Simulation Technology (CST) Studio 2023. The system design without metamaterials achieved a gain of 5.28 dBi and a bandwidth of 353.0 MHz. The integration of the CSRR led to an improvement in gain, 5.39 dBi at 3.8 GHz, which is above most of the literature reviewed, although there was a slight reduction in bandwidth to 135.2 MHz. The objectives of achieving a CMSA design with a gain between 5 to 10 dBi while maintaining a compact size were accomplished. Despite the slight reduction in bandwidth observed when integrating the CSRR into the CMSA, the overall results highlight the significant role metamaterials played in enhancing the performance of microstrip antennas for 5G technology applications.*

Keywords: *Antenna Performance, Circular Microstrip Antenna (CMSA), Complementary Split Ring Resonator (CSRR), Fifth Generation (5G) Communications, Metamaterials*

1. INTRODUCTION

Antenna plays very significant role in wireless communication systems including terrestrial and satellite communication networks [1,2,3,4]. Fifth-generation (5G) wireless communication systems provide significant improvements in data rates [5] latency and reliability compared to fourth-generation (4G) [6,7, 8,9]. To achieve these improvements, 5G utilizes a wider range of frequency bands, including the ultra-wideband (UWB) spectrum from 3.1 to 10.6 GHz [10, 11, 12].

Microstrip antennas (MSAs) are preferred for 5G applications due to their low profile, lightweight, and ease of fabrication. However, conventional MSAs have a narrow bandwidth, limiting their use in UWB systems [13]. To address this limitation, various approaches have been proposed in the literature. For example, Kim and Yang [14] designed a miniaturized circular microstrip antenna (CMSA) for wearable applications, achieving good performance at 2.4 GHz by using a flexible substrate and a meandered slot design. Similarly, introduction of superstrate layer to enhance the radiation efficiency and gain of CMSAs, achieved a gain improvement of 3 dB with good efficiency [15].

Despite these advancements, conventional microstrip antennas still face challenges in accommodating Nigeria's UWB frequency range (3.1 to 10.6 GHz), which is essential for high-speed data transmission in applications such as wireless USB, radar imaging, and real-time location systems [16]. To overcome these challenges, metamaterials—artificial materials with unusual electromagnetic properties—are introduced to provide negative permittivity and permeability. Metamaterial-based antennas can achieve wider bandwidths than conventional microstrip antennas, making them suitable for UWB applications [17]. The circular microstrip antennas (CMSAs) with metamaterials are particularly attractive for 5G UWB applications due to their omnidirectional radiation pattern and compact size [18, 19, 20].

Although metamaterial-based CMSAs envisage good applications for 5G, there is still a need to further improve their performance in terms of bandwidth, gain, and radiation efficiency [21]. This research investigates the use of metamaterials to enhance the performance of CMSAs for 5G UWB services. Specifically, the study aims at improving the impedance bandwidth to cover the 5G UWB band allocated for mobile telecommunication and satellite communication in Nigeria (3.4 to 4.2GHz), improve the gain, radiation efficiency, and reduce the antenna's size. The proposed antenna design is evaluated using Computer Simulation Technology (CST) Studio Suite 2023 software. The success of this research will contribute to the development of high-performance metamaterial-based CMSAs for 5G UWB systems, enhancing the deployment of 5G UWB services in Nigeria for improved quality of experience.

2. DESIGN METHODOLOGY

2.1 Design of Circular Microstrip Antenna:

A single-element circular microstrip antenna is designed according to Balanis [22]. The primary requirement is the CMSA without metamaterial. Thereafter, emphasis is converged on the design of a CSRR of the metamaterial-based circular microstrip antenna. In the design process of a Circular Microstrip Antenna, some parameters such as resonant frequency (f_r), substrate thickness (h) and relative dielectric constant (εr) are very significant. Some structural parameters such as circular patch radius (a), substrate length (L), substrate width (W) and feed line inset distance (Fi) are also calculated. The radius of the circular patch is expressed as Balanis [22]. The Circular microstrip antenna is designed based on the cavity model formulation for the dominant TMz110 mode [22, 23].

i. **Operating frequency:** The resonant frequency (f_r) of the antenna are determined appropriately. The operating frequency of the proposed antenna range from 3.4 GHz to 4.2 GHz. The resonant frequency selected for the design was 3.8GHz because the proposed antenna is designed for 5G UWB applications.

ii. **Substrate:** The height (h) of the substrate is between $0.003\lambda 0 \leq h \leq 0.05\lambda 0$ and its dielectric constant (εr) is commonly in the range $2.2 \leq \varepsilon r \leq 12$ [22]. The performance of microstrip antennas depends on a balancing act between substrate thickness and dielectric constant. While thicker substrates with lower dielectric constants (ε_r) generally lead to improved radiation characteristics, wider bandwidth, and higher efficiency, they also result in larger antenna sizes. Conversely, thinner substrates with higher εr decrease the fringing fields, resulting in higher resonant frequencies and smaller antenna sizes. According to Balanis [22], the height of the substrate is determined by the wavelength of the operating frequency using the equation below:

$$h \leq 0.3\, x \frac{\lambda_0}{2\pi\sqrt{\varepsilon_r}} \tag{1}$$

and

$$\lambda_0 = \frac{c}{f_r} \tag{2}$$

where $\boldsymbol{c}$ is the speed of light = 3×10^8 m/s, and f_r is the selected resonant frequency (3.8 GHz), and λ_0 is the wavelength in free space. The proposed substrate used for the antenna is FR-4 (lossy) with a dielectric constant (ε_r) of 4.4, loss tangent ($\tan\delta$) of 0.019, and a resonant frequency (f_r) of 3.8 GHz, respectively. The height of the substrate is determined from Equation (1) and (2) as:

$\lambda_0 = \frac{3\ X10^8}{3.8\ X\ 10^9}$ = 78.95 mm

$h \leq 0.3\, x \frac{0.07895}{2\pi\sqrt{4.4}}$ = 1.797 mm

Thus, substrate height (h) was chosen as 1.6 mm in line with the range of values calculated for height from Equation (1) A substrate with a high dielectric constant has been selected to further reduce the dimensions of the antenna. The resonance frequency, f_r is given as [22]:

$$fr = \frac{1.8412\ c}{2\pi a\sqrt{\varepsilon r}} \tag{3}$$

$$fr = \frac{1.8412\ x\ 3.0{*}10\text{^}8}{2{*}3.142{*}10.58{*}\sqrt{4.4}} = 39.612\ \text{GHz}$$

Where $\boldsymbol{c}$ is the speed of light in free-space and $\boldsymbol{a}$ is the radius of the microstrip antenna.

iii. **Determination of the radius of the circular patch:** The circular microstrip patch antenna (CMSA) is designed to suits certain applications. It occupies less space compared to a rectangular patch antenna operating at the same frequency. The formula for computation of the circular microstrip radius is given by the Equation (2) [9].:

$$a = \frac{F}{\left\{1+\frac{2h}{\pi\varepsilon rF}\left[ln\left(\frac{\pi F}{2h}\right)+1.7726\right]\right\}^{1/2}} \tag{4}$$

where F is given as:

$$F = \frac{8.79\ x\ 10^9}{fr\sqrt{\varepsilon r}} \tag{5}$$

hence, $F = \frac{8.79\ x\ 10^9}{3.8\ x\ 10^9\sqrt{4.4}} = 1.103$

therefore, the radius, $a = \frac{1.1}{\left\{1+\frac{2x1.6}{\pi\ x\ 4.4\ x\ 1.1}\left[ln\left(\frac{\pi\ x\ 1.1}{2\ x\ 1.6}\right)+1.7726\right]\right\}^{1/2}}$ = 10.57723 mm

As a result of the effect of fringing, the electrical radius extends slightly beyond the physical radius. This makes the effective radius, a_e to be:

i. $$a_e = a\left\{1 + \frac{2h}{\pi a\varepsilon r}\left[\ln\left(\frac{\pi a}{2h}\right) + 1.7726\right]\right\}^{1/2} \tag{6}$$

where:

f_r = Resonance frequency, ε_r = Substrate's Relative Permittivity, h = Substrate height, a = Physical Radius of the Patch, and a_e = Effective Radius.

$$a_e = 10.577\left\{1 + \frac{2x1.6}{\pi x10.577x4.4}\left[\ln\left(\frac{10.577\pi}{2x1.6}\right) + 1.7726\right]\right\}^{1/2} = 11.043 \text{ mm.}$$

In this design, FR-4 (lossy) substrate is examined. The dielectric constant, the height of the substrate, the radius of the microstrip, and the effective radius are tabulated below. The centre frequency for the frequency range of between 3.4 GHz and 4.2 GHz is taken as 3.8 GHz. The effective diameter of the microstrip is tabulated in Table 1.

Table 1: Substrate parameter for system design

Substrate	Dielectric Constant, Ɛr	Height (mm)	Radius, A (mm)	Effective Radius, a_e (mm)	Effective Diameter, d_e (mm)
FR-4	4.40000	1.60000	10.57723	11.04304	22.08608

A.

2.2 Determination of the Feed Line Parameters

For circular microstrip antenna, the feed line dimension is between 0.3a to 0.5a, where a is the radius of the circular patch. The feed line of a circular microstrip antenna (CMSA) was designed after the dimensions of the patch were finalized. For CMSAs with microstrip feed lines, the conductive strip is typically connecting directly to the periphery of the circular patch. A quarter-wave transmission line with a characteristic impedance (Z_1) connected the CMSA to a microstrip transmission line with a characteristic impedance of Z_0 = 50 Ω. This matching technique ensures an efficient energy transfer from the antenna's input impedance to the feed line to minimize the signal reflection and power loss towards the transmission line. If R_{in} represents the input edge impedance of the antenna, then the characteristic impedance of the quarter-wave transformer (Z_1) can be calculated as:

$$Z_1 = \sqrt{Z_0 R_{in}} \tag{7}$$

where Z_1 is the impedance of the quarter-wave transformer, Z_0 is the characteristic impedance of the microstrip feed line, and R_{in} is the input edge impedance of the antenna.

For effective integration of the patch onto the substrate, the width of the feed must be less than the diameter of the circular patch. Modifying the width of the quarter-wave strip allows for adjustments to Z_1. As the width of the microstrip line increases, its characteristic impedance (Z_0) decreases. To ascertain the resonant input impedance, the conductance of the slots is initially determined. An approximation for calculating the resonant input edge resistance (Rin) of the patch is provided by:

$$\text{Rin} = \frac{1}{2(G1 \pm G12)}\Omega \tag{8}$$

where G_1 represents the self-conductance of a single slot with finite width, and G_{12} stands for the mutual conductance between two slots. For CMSAs, considering the transmission line model, the mutual conductance G_{12} is typically small and can be disregarded. This model approximates the impedance at the feed point of the microstrip by treating the edges of the circular patch as slots represented by a parallel equivalent admittance Y (comprising conductance G and susceptance *B*).

Determining the input edge impedance of a patch antenna presents a challenge due to the complex interaction between its geometry and electromagnetic fields. One approach to determine the transformer input impedance [24]:

$$\text{Zin} = \frac{\eta}{2W\sqrt{\varepsilon_{r-1}}} \tag{9}$$

where: Zin: input impedance at the edge (Ω), η: intrinsic impedance (≈ 120π Ω for free space), W: width of the patch (m) = 3.8 mm and εr: Dielectric constant of the substrate = 4.4

$$\text{Zin} = \frac{120*3.143}{2*38*\sqrt{3.4}} = 26.9\ \Omega.$$

For the design, the Software, CST Studio Suite, 2023 edition, is used to model the antenna and calculation of input impedance:

i. **Calculation of the width of the feed line (W):** The width of the feed line for a desired characteristic impedance (Z_0) in a microstrip line can be calculated using Wheeler's formula, which provides a good approximation for W. For a microstrip line over a substrate with an effective dielectric constant εeff and a substrate height h, the width (W) can be calculated from: when $Z_0 < (60)/(\varepsilon_{eff})$ (which is usually the case for 50Ohms in typical substrates like FR-4):

$$W = \frac{W_f}{h} = \frac{8e^A}{e^{2A}-2} \tag{10}$$

Where, W_f is the feed line width, h is the substrate height = 0.0016 m, and

$$A = \frac{Z_0}{60}\sqrt{\frac{\varepsilon_{eff}+1}{2}} + \frac{\varepsilon_{eff}-1}{\varepsilon_{eff}+1}\left(0.233 + \frac{0.11}{\varepsilon_{eff}}\right) \quad (11)$$

$$A = \frac{50}{60}\sqrt{\frac{3.33+1}{2}} + \frac{3.33-1}{3.33+1}\left(0.233 + \frac{0.11}{3.33}\right)$$

A = 1.363

Hence,

$$W = \frac{8e^{1.244}}{e^{2*1.244} - 2}$$

W = 2.356

$W_f/0.0016 = 2.356$

$W_f = 2.356 * 0.0016 = 0.0038$ m = 3.8 mm.

Moreover, to achieve 50 Ω characteristic impedance, for the rectangular microstrip antenna, it was discovered from the CST studio software that the width of the feeding line must be 3.083mm. This was applied to the circular patch for simulation evaluation.

ii. Calculation of the quarter wavelength of the feed line: the length of the quarter wave transmission line, L_Q is given by [22,23] as:

$$L_f = \frac{\lambda}{4} = \frac{\lambda_0}{4\sqrt{\varepsilon_{reff}}} \quad (12)$$

$$\lambda_0 = \frac{c}{f_r} = \frac{3\ X10^8}{3.8 \times 10^9} = 0.07895 \text{ m}$$

Thus, $L_f = \frac{0.07895}{4\sqrt{3.33}} = 10.82\ mm$

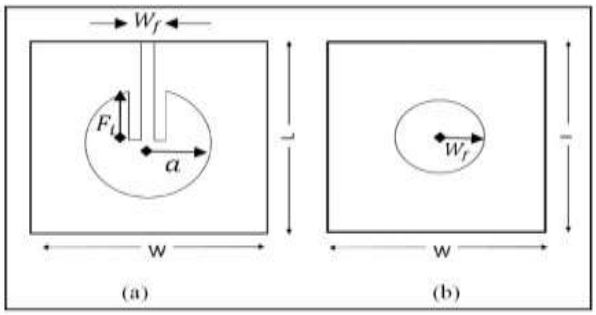

Figure 1: The front and back view of the circular microstrip antenna.

iii. Determination of the 50 Ω microstrip feed line length: Based on the literature [23], the length of a microstrip transmission line L_0 is adjusted on the CST Studio software to arrive at a value that gives optima efficiency. For this design, $L_0 = 8.58$ mm. Table 2, shows the dimensions of the system design and simulated circular microstrip antenna using FR-4 (lossy) as the substrate.

Table 2: Dimensions of the system design.

Design Parameter	Values
Patch dimensions:	
Radius (r)	10.580 mm
Dielectric constant (ε_r)	4.400
Substrate height (h)	1.600 mm
Patch thickness (t)	0.036 mm
Ground plane dimensions:	
Ground plane radius (r_g)	21.160 mm
Feed line dimensions:	
Width of 50 Ω transmission line (W_0)	3.083 mm
Length of 50 Ω transmission line (L_0)	19.740 m
Input edge impedance of the patch (R_{in})	26.9 00Ω
The characteristic impedance of the feed line (Z_0)	50.0 Ω

B. 2.3 Metamaterial Design

i. Split Ring Resonator: the schematic diagram of the SRR is shown in Figure 3. The resonance frequency is given as [22]:

$$f_0 = \frac{1}{2\pi}\sqrt{\frac{2}{(C_0 + C_g)L}} \tag{13}$$

where c_o is the distributed capacitance, Cg is the gap capacitance and L is the self-inductance of the rings.

$$L = \mu_0 r\left(ln\frac{8r}{w} - \frac{7}{8}\right) \tag{14}$$

The gap capacitance Cg is calculated as a parallel-plate capacitance with a fringing field correction term.

$$Cg = \varepsilon 0\left[\left[\frac{hw}{g} + (h + w + g)\right]\right] \tag{15}$$

w is the width of the metallic ring and h is its thickness; g = g_1 = g_2 is the split gaps, r is the SRR mean radius formulated as:

$$r = r + w + d/2 \tag{16}$$

where d is the inter ring spacing and r is the inner ring radius. The mutual (distributed) capacitance is demonstrated as:

$$C_0 = \pi r C_{pul}. \tag{17}$$

where C_{pul} is per unit length capacitance which is also calculated as:

$$C_{pul} = \varepsilon_0 \varepsilon_e F(k) \tag{18}$$

$$\varepsilon_0 = 1 + \frac{(\varepsilon_r - 1)F(k)}{2F(k1)} \tag{19}$$

$$k = a/b;\ a = d/2;\ \text{and}\ \ b = d/2 + w \tag{20}$$

$$k' = \sqrt{1 - k^2} \tag{21}$$

where k' is wave effective number which represents the effective propagation constant of the electromagnetic wave within the SRR's conductive strip. k is the wavenumber in free space. $\varepsilon_0 = 8.85 * 10^{-12}$ is the permittivity of free space, ε_r is the dielectric constant of the material and t is the substrate thickness.

$$k_1 = \frac{sinh\left(\frac{\pi a}{2t}\right)}{sinh\left(\frac{\pi b}{2t}\right)} \tag{22}$$

k_1 = characteristic impedance factor. k_1 accounts for the impedance mismatch between the SRR's strip and the surrounding medium (usually air). It arises due to the abrupt change in geometry at the strip's edges. The values a, b and t refers to the radius of the SRR, the inner radius of the SRR and the thickness of the strip respectively and $F(k)$ is given by Equation (21):

$$F(k)\begin{cases} \frac{1}{\pi} ln2\frac{1+\sqrt{k'}}{1-\sqrt{k'}} & , \quad 0 < k \le \frac{1}{\sqrt{2}} \\ \pi ln\left(2\frac{1+\sqrt{k}}{1-\sqrt{k}}\right)^{-1} & , \quad \frac{1}{\sqrt{2}} < k \le 1 \end{cases} \tag{23}$$

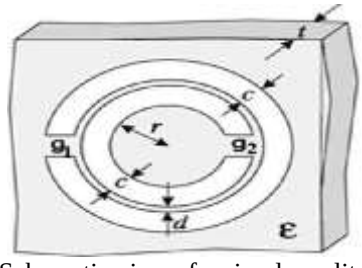

Figure 2: Schematic view of a circular split ring resonator [23]

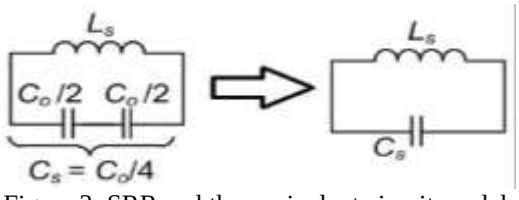

Figure 3: SRR and the equivalent circuit model.

ii. Complimentary split ring resonator: Complementary Split Ring Resonators (CSRRs) is used in this design. It represents a pivotal advancement in the domain of metamaterials, particularly influencing microwave and antenna engineering. Initially conceptualized by [25] for achieving negative permeability, CSRRs have been widely adopted for filtering and miniaturization purposes in microwave circuits and antennas. CSRRs are essentially the inverse of Split Ring Resonators (SRRs); they consist of etched concentric ring slots on a planar substrate. When these structures

are excited by an electromagnetic field, they exhibit a negative effective permittivity within a specific frequency range, leading to unique electromagnetic properties not found in natural materials [12]. One of the foremost applications of CSRRs is in the design of compact and efficient filters for microwave circuits. By embedding CSRRs into microstrip lines or patch antennas, engineers can achieve miniaturization, enhance bandwidth, and improve selectivity [25]. Furthermore, CSRRs have been instrumental in the development of novel antenna designs, offering solutions for size reduction without compromising performance—critical for modern wireless communication systems [25]. The integration of CSRRs into microwave and antenna design provides several advantages, miniaturization, enhanced bandwidth and selective filtering.

2.4 Design of Metamaterial-Based Circular Microstrip Antenna

To calculate the dimension of the metamaterial, the resonance frequency must be known. For this research work, the frequency range is between 3.4 GHz to 4.2 GHz. Therefore, 3.8 GHz is set as the middle frequency. To design a Complementary Split Ring Resonator (CSRR) for 3.8 GHz, with a substrate having a relative permittivity (εr) of 4.4 and a thickness (h) of 1.6 mm, several factors are considered. The design process involves calculating the outer radius, inner radius, and the gap of the CSRR structure. A general approach is outlined based on electromagnetic theory and resonant condition considerations.

i. **Determine the effective permittivity (ε_{eff}):** The effective permittivity accounts for the dielectric substrate's impact on the wave's propagation speed. It can be estimated for a microstrip line, which is similar in structure to the substrate part of a CSRR, using the formula:

$$\varepsilon_{eff} = \frac{\varepsilon_r+1}{2} + \frac{\varepsilon_r-1}{2}\left(\frac{1}{\sqrt{1+12\frac{h}{W}}}\right) \quad (24)$$

where $\boldsymbol{W}$ is the width of the CSRR. Since CSRR does not have a specific "width" like a microstrip line, this formula is more indicative and the actual ε_{eff} might be derived from full-wave simulations for accurate design. From the CST Studio software, ε_{eff} is found to be 3.3.

ii. **Estimate the guided wavelength (λg):** The guided wavelength on the substrate is different from the free-space wavelength due to the dielectric medium and can be estimated as:

$$\lambda_g = \frac{\lambda_0}{\sqrt{\varepsilon_{eff}}} = \frac{0.079}{\sqrt{3.3}} = 0.0434\ m = 43.4\ mm \quad (25)$$

where λ_0 is the free-space wavelength, $\lambda_0 = c/f_0$, with c being the speed of light (3×10^8 m/s) and f_0 the resonant frequency (3.8 GHz in this case):

$$\lambda_0 = \lambda_0 = \frac{c}{f_0} = \frac{3.0\ x\ 10^8}{3.8\ x\ 10^9} = 0.079\ \text{m}$$

iii. **CSRR dimension estimates:** The actual dimensions of a CSRR depend on the targeted resonant frequency, substrate properties, and the desired coupling strength. A starting point for the dimensions can be derived from empirical formulas or, more commonly, from parametric studies and optimizations using CST Studio. A common approach is to start with dimensions that are a fraction of the guided wavelength (λg), adjusting for the desired resonant frequency:
   1. Outer Radius (R_o): A fraction of λg, e.g., λg/4 to λg/10, as a starting point.
   2. Gap (g): The gap width influences the resonance's frequency and quality factor. A smaller gap can lead to higher quality factors. The starting values is 0.5 mm, adjusted based on simulation results.
   3. Inner Radius (Ri): This can be determined based on the desired outer radius and gap width, keeping in mind the structural integrity and fabrication capabilities.
   4. The final value as adjusted during simulation is indicated in Table 2.

Table 2: Metamaterial dimension

Parameter	Value (mm)
Outer Radius R	4.34
Gap, s	0.50
Space u	0.50
Inner Ring r	3.34
Ring's width, q	0.50

Using the above parameters, the inductance, L of the SRR is 11.3388 nH and the capacitance = 154.544 fF (154.544 femtofarads).

The challenge of getting appropriate feed line in the design was resolved using error checking method during simulation. The Circular Microstrip Antenna and the final feed line parameters are given in Table 3.

Table 3: The final dimension of the system esign

Parameters	Dimension (mm)
Substrate length	50.580
Substrate Breadth	21.160
Substrate Thickness	1.600
Ground plane Diameter	42.320
Ground Plane Thickness	0.036
Circular Patch Diameter	21.160
Circular Patch Thickness	0.036
Feed line Width	3.083
Feed line Length	18.260

CSRR	Dimension (mm)
Outer Ring	4.000
Gap, s	0.500
Space, u	0.500
Ring width, q	0.500
Inner Ring	3.000

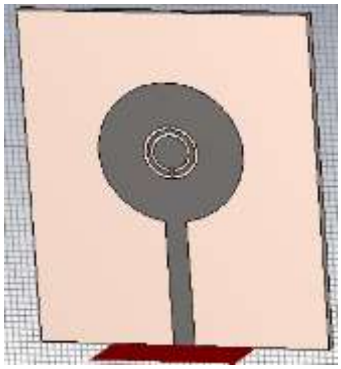

Figure 4 (a): Circular patch

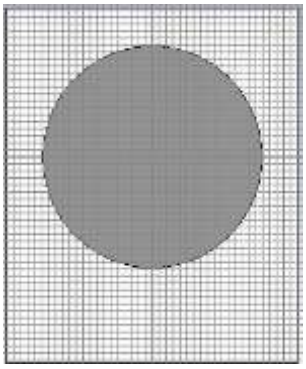

Figure 4 (b): Ground plane

3. RESULTS AND DISCUSSION

To assess the bandwidth of the two antennas, one with metamaterial (MTM) and one without (Non-MTM) metamaterial, the respective Voltage Standing Wave Ratio (VSWR) and reflection coefficient (S1,1) values across the frequency range provided was assessed. In the context of antenna design, bandwidth typically refers to the range of frequencies over which the antenna performs satisfactorily, commonly defined by a VSWR less than 2 or a return loss (S1,1) better than -10 dB. [11]

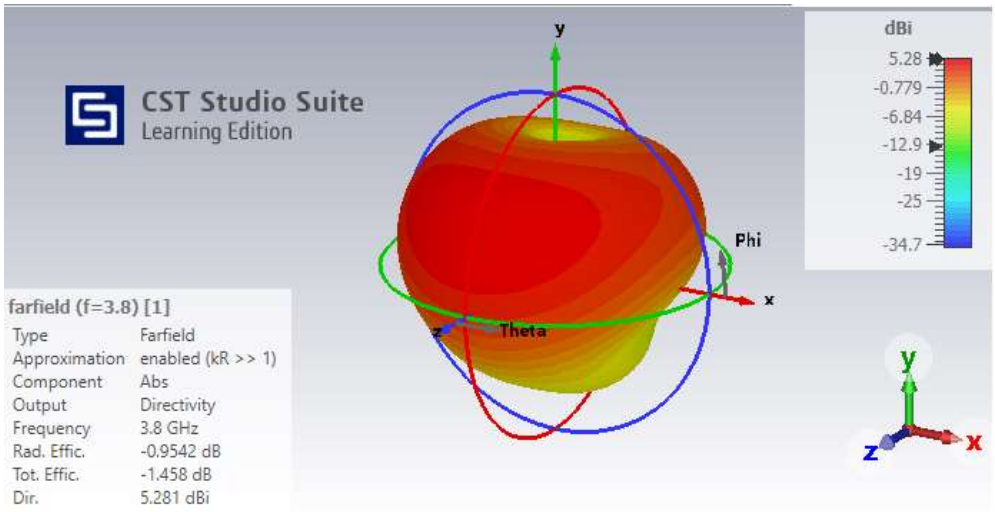

Figure 5: Gain of 5.28dBi at 3.8 GHz single band antenna (Non-MTM CMSA)

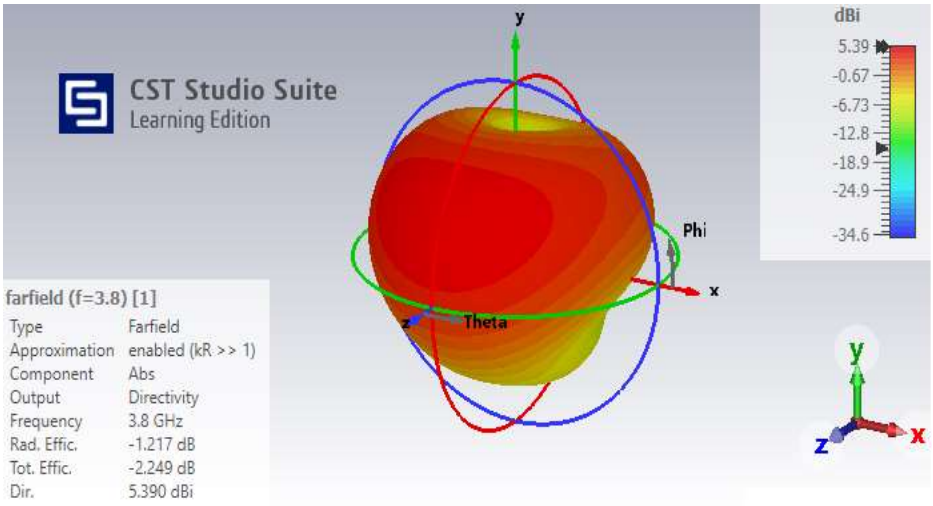

Figure 6: Gain of 5.39dBi at 3.8 GHz of proposed MTM-CMSA

3.1 Analysis of Simulation Results:

i. **VSWR data:** For the CMSA without MTM, the VSWR remains below 2 from about 3.5 GHz to 3.8 GHz, indicating a narrow bandwidth (300 MHz approx.) The VSWR peaks to values higher than 3.0 as frequency increases, reaching up to 5.36 at 4.2 GHz, showing poor performance outside the aforementioned narrow band. When metamaterial is incorporated, the VSWR stays below 2 from approximately 3.5 GHz to 3.68 GHz, similar to the Non-MTM case, indicating a narrow bandwidth of approx. 168 MHz. However, the VSWR is generally higher across the range with MTM, spiking to values as high as 7.65 at 4.1 GHz, suggesting worse performance at higher frequencies compared to the Non-MTM setup.

Table 4: The VSWR Performance at different frequencies

Frequency	VSWR (Non MTM)	VSWR (MTM)
3.400	2.005	3.450
3.500	1.745	2.106
3.516	-	2.000
3.600	1.649	1.798
3.686	-	2.000
3.700	1.736	2.059
3.800	1.989	2.702
3.900	2.396	3.876
4.000	3.006	5.902
4.100	3.980	7.650
4.200	5.360	5.482

The Voltage Standing Wave Ratio (VSWR) tables for a circular microstrip antenna without and with metamaterial (MTM) across a range of frequencies provide additional insight into the antenna's performance and the effect of incorporating metamaterial into its design.

ii. **S1,1 Parameter Data:** Without metamaterial, the CMSA Shows a progressive improvement in reflection coefficient as frequency increases, starting from -9.513 dB at 3.4 GHz to -3.28 dB at 4.2 GHz. Best performance (lowest reflection) around 3.6 GHz to 3.7 GHz with values nearing -12.222 dB, aligning with the VSWR findings. With metamaterial incorporated, the reflection coefficients are generally poorer across the board compared to Non-MTM, with values ranging from -5.219 dB at 3.4 GHz to -3.205 dB at 4.2 GHz. The reflection coefficient shows a notable deterioration, especially at 3.8 GHz and higher frequency.

4. CONCLUSION

In this research work, metamaterial-based CMSA (CMSA-MTM) and non-metamaterial CMSA (Non-MTM) were studied for 5G applications. Both antenna system designs operate within the frequency range of 3.4 GHz to 3.800 GHz, it is observed that the inclusion of metamaterials influences the impedance characteristics of the antenna, due to its interaction with the antenna's near field. Generally, while the directivity of the system design is slightly higher with MTM, it has been observed that bandwidth degraded with the inclusion of metamaterials. This could be due to the specific properties of the MTM affecting the resonant behaviour of the antenna system. The narrow bandwidth of both antennas

limits their application flexibility, though without MTM, the antenna demonstrates slightly better gain and less volatile response across the studied frequency range.

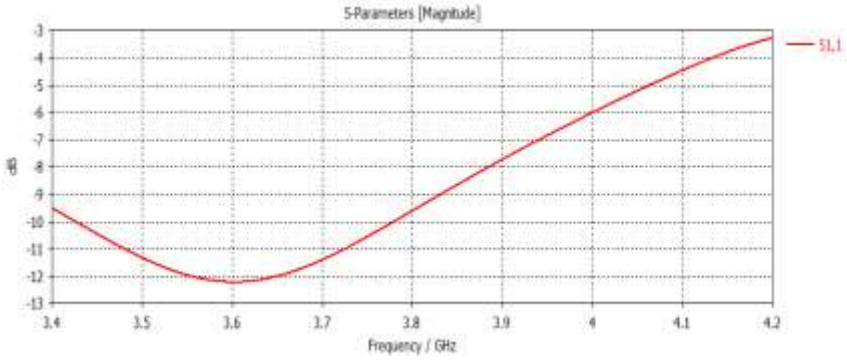

Figure 7: S-parameter of the Designed CMSA without MTM

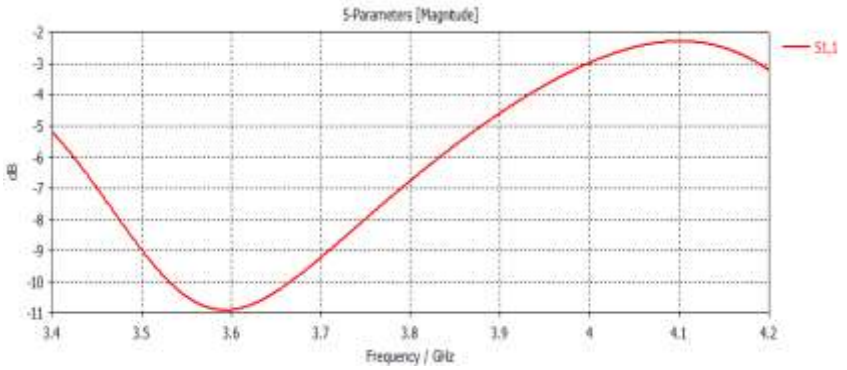

Figure 8: S-parameter of the Designed CMSA with MTM

However, the proposed design has achieved gain of 5 to 10 dBi while maintaining a compact profile. The design antenna is more applicable where a high directivity with a narrower bandwidth might be beneficial, such as in directional communication systems [26], radar, or in environments where channel specificity is crucial to avoid interference [27]. Though several metamaterial-based microstrip antennas have previously been discussed in the literature, the novel geometry presented in this research work covers the approved C-band 5G deployment frequency for the Nigerian market while maintaining a small, compact, planar profile making it suitable for portable devices.

REFERENCES

[1] Akwaowo, U., Ubom, E., Ukommi, U. & Obot, A., (2023). Design of a Rectangular Microstrip Antenna Resonating at 3.5 GHz for Future Wireless Networks. Science and Technology Publishing (SCI & TECH), 7(12), 1593- 1597.

[2] Ukommi, U, Ekanem, K, Ubom, E & Udofia, K (2024). Evaluation of Rainfall Rates and Rain-Induced Signal Attenuation for Satellite Communication in the South-South region of Nigeria. Nigerian Journal of Technology (NIJOTECH), 42(4), 472-477.

[3] Ekanem, K, Ubom, E. & Ukommi U. (2022). Analysis of Rain Attenuation for Satellite Communication in Akwa Ibom State, Nigeria. The Nigerian Institute of Electrical and Electronic Engineering (NIEEE) Proceedings of the International Conference and Exhibition on Power and telecommunication (ICEPT 2022), 23-24.

[4] Essien, A., Ukommi, U., & Ubom, E. (2024). Downlink power budget and bit error analysis for LoRa-based sensor node-to-satellite link in the industrial, scientific and medical frequency bands. In Signals and Communication Technology (pp. 143–152). Springer Nature, Switzerland. https://doi.org/10.1007/978-3-031-53935-0_14

[5] Ubom, E., Akpanobong, A., & Ukommi, U. (2019). Spectrum Occupancy in Rural Nigeria: A Case for a lightly Licensed Spectrum Bandfor Rural Broadband Enhancement. International Journal of Computer Science & Information Technology (IJCSIT), 11(4), 81- 99.

[6] Ukommi, U., Kodikara A., Dogan, S., & Kondoz, A. (2013). Content-Aware Bitrate Adaptation for robust mobile video services. IEEE International Symposium on Broadband Multimedia Systems and Broadcasting (BMSB), London, UK, 1-4, doi: 10.1109/BMSB.2013.6621696.

[7] Udoh, R, Ukommi, U & Ubom, E (2023). Evaluation of Modified Artificial Neural Network-Based Interference Mitigation In 5G Network. Science and Technology Publishing (SCI & TECH), 7(12), 1604-1613.

[8] Umoh, V., Ukommi, U., & Ekpe, M. (2022). A Comparative Study of User Experienced Mobile Broadband Performance. Nigerian Journal of Technology (NIJOTECH), 41(3), 560-568.

[9] Ukommi, U. (2024). Assessing the Impact of Media Stream Packet Size Adaptation on Wireless Multimedia Applications. *ABUAD Journal of Engineering Research and Development*, *7*(1), 221-230. https://doi.org/10.53982/ajerd.2024.0701.23-j
[10] Uloh, C., Ubom, E., Obot, A., & Ukommi, U. (2024). Interference Mitigation and Power Consumption Reduction for Cell Edge users in Future Generation Networks. Journal of Engineering Research and Reports, 26(2), 89-106.
[11] Udoh, R, Ukommi, U & Ubom, E (2023). Interference Mitigation In 5G Network Using Frequency Planning and Artificial Neural Network (ANN). Journal of Multidisciplinary Engineering Science and Technology (JMEST), 10(12), 16534- 16540.
[12] Chen, H., Yuan, W., & Huang, Y. (2021). Design of a metamaterial-based ultra-wideband circular microstrip antenna for 5G applications. IEEE Trans. Antennas Propag. 70(1), 505-513.
[13] Liu, Z., Sharma, S.K., & Gupta, Y.M. (2007). A Survey of Microstrip Patch Antenna Design Techniques for UWB Applications. Prog. Electromagn. Res. 79, 373-414.
[14] Kim, H., & Yang, B. (2018). Miniaturized circular microstrip antenna for wearable applications. IEEE Antennas Wireless Propag. Lett. 17(5), 789-793.
[15] Kumar, V., & Patel, D. (2019). High-efficiency circular microstrip antenna with superstrate layer. International Journal of Antennas and Propagation.
[16] Federal Communications Commission (2002). First Report and Order, Revision of Part 15 of the Commission's Rules Regarding Ultra-Wideband Transmission Systems.
[17] Bahrami, H., Alibakhshikenari, M., Virdee, B.S., & Antoniades, M.A. (2014). Metamaterial-based UWB Antennas for Wireless Communication Systems. IEEE Antennas Propag. Mag., 58(4), 106-123.
[18] Mishra, S.K., Ranjan, R.K., & Kumar, P. (2023). Metamaterial-based Circular Microstrip Antenna for 5G UWB Applications. IEEE Access, 11, 65836-65848.
[19] Hossain, M.S., Rahman, M.A., & Islam, M.T. (2022). Design and Analysis of Metamaterial-loaded Circular Microstrip Antenna for 5G UWB Applications. Int. J. Antennas Propag., 2022, Art. no. 7195497.
[20] Singh, A.K., Rajput, A.S., & Shrivastava, V.K. (2021). Enhancing the Bandwidth and Radiation Characteristics of a Circular Microstrip Antenna Using Metamaterials for 5G UWB Applications. Int. J. Microw. Wireless Technol., 13(10), 1382-1391.
[21] Kumar, A., Saini, M., & Kumar, P. (2022). A compact metamaterial-based circular microstrip antenna for 5G UWB applications. Microw. Opt. Technol. Lett. 64(11), 1857-1864.
[22] Balanis, C.A. (2005). Antenna Theory: Analysis and Design, 3rd edn. John Wiley & Sons, New York.
[23] Long, S.A., McAllister, M.W., & Shen, L.C. (1983). The resonant cylindrical dielectric cavity antenna. IEEE Trans. Antennas Propag. 31(3), 406-412.
[24] Pozar, D.M. (2012). Microwave Engineering, 4th edn. John Wiley & Sons, New York.
[25] Pendry, J.B., Holden, A.J., Robbins, D.J., & Stewart, W.J. (1999). Magnetism from conductors and enhanced nonlinear phenomena. IEEE Trans. Microw. Theory Techn. 47(11), 2075-2084.
[26] Ukommi, U., & Ubom, E. (2023). Impact Assessment of Elevation Angles on Signal Propagation at VHF and UHF Frequencies for Improved Rural Telephony. *ABUAD Journal of Engineering Research and Development*, *6*(2), 136-142.
[27] Olufemi, O. I., & Ukommi, U. (2024). Evaluation of energy consumption and battery life span for LoRa IoT multisensor node for precision farming application. Signals and Communication Technology. Springer Nature, Switzerland. https://doi.org/10.1007/978-3-031-53935-0_15